

New measurement of the astrophysically important $^{40}\text{Ca}(\alpha, \gamma)^{44}\text{Ti}$ reaction

D. Robertson,* J. Görres, P. Collon, and M. Wiescher

Department of Physics, University of Notre Dame, Notre Dame, Indiana 46556, USA

H.-W. Becker

RUBION, Ruhr-Universität Bochum, Universitätsstrasse 150, D-44780 Bochum, Germany

(Received 23 September 2011; revised manuscript received 5 April 2012; published 27 April 2012)

The relatively short-lived radionuclide ^{44}Ti is of considerable importance for the interpretation of nucleosynthesis in core-collapse supernova environments. Production is predominantly through the $^{40}\text{Ca}(\alpha, \gamma)^{44}\text{Ti}$ reaction, which has been studied in this work over the energy range $E_{\text{cm}} = 2.73\text{--}4.18$ MeV, via direct γ counting and the 4π -summing technique, utilizing a previously characterized 12 inch \times 12 inch single NaI crystal. The inferred reaction rate is compared here to both current experimental measurements and theoretical model calculations.

DOI: [10.1103/PhysRevC.85.045810](https://doi.org/10.1103/PhysRevC.85.045810)

PACS number(s): 26.30.-k, 25.55.-e, 27.40.+z, 97.60.Bw

I. INTRODUCTION

The discovery along the galactic plane of radioactivity associated with long-lived γ emitters, via satellite based observatories from COMPTEL to INTEGRAL, has opened a new window into the study and interpretation of the nucleosynthesis of massive stars during their last stages of stellar evolution, and explosive nucleosynthesis in the expanding shock front of a core-collapse supernova. The measurement of the ^{26}Al ($t_{1/2} = 7.17 \pm 0.24 \times 10^5$ yr) 1.81 MeV γ -source distribution, demonstrated the direct association between the production of this long-lived isotope and the continuously on-going nucleosynthesis in massive stars along our galaxy [1]. Other long-lived γ sources discovered include ^{60}Fe ($t_{1/2} = 2.62 \pm 0.04 \times 10^6$ yr), where the 1.17 and 1.33 MeV lines from the decay of the ^{60}Co daughter nucleus have been observed with RHESSI and INTEGRAL, and ^{44}Ti ($t_{1/2} = 58.9 \pm 0.3$ yr), where the 1.157 MeV γ line associated with the decay of the ^{44}Ca isotope has been discovered by INTEGRAL in the supernova remnants Cassiopeia A [2] and Vela [3]. These discoveries have led to a flurry of simulations regarding the production of these long-lived isotopes to use them as signatures for monitoring late star evolution and type II a core-collapse nucleosynthesis. These models require reliable rates for the production and depletion of these isotopes for a wide range of stellar temperatures. This has led to new experimental efforts in determining the associated thermonuclear reaction and decay rates.

The case of ^{44}Ti is a particularly interesting one because the radioactive decay of ^{44}Ti has significant observational consequences for the light curves of core-collapse supernovae [4], and the observed ^{44}Ti to ^{56}Ni ratios are higher than predicted by standard core-collapse supernova model simulations [5,6]. It is therefore of particular interest to understand the production mechanism, which typically is assumed to be associated with the α -rich freeze-out phase of the expanding shock front [7]. A number of reaction-rate sensitivity studies have been performed in the broader framework of model parametrization for the α -rich freeze-out expansion phase [8,9], seeking to

identify the role of critical reaction rates for ^{44}Ti production at thermal equilibrium and quasiequilibrium conditions. A recent parameter study [10] uses different expansion trajectories to investigate the role of particular reactions decoupling from equilibrium. All these studies highlight the relevance of the $^{40}\text{Ca}(\alpha, \gamma)$ radiative capture reaction as the main production link for the ^{44}Ti radioisotope.

There have been a significant number of experiments over the last 40 years trying to determine a reliable thermonuclear reaction rate for the $^{40}\text{Ca}(\alpha, \gamma)^{44}\text{Ti}$ reaction using a number of different experimental techniques, ranging from gamma counting studies (e.g., Ref. [11]), to the use of accelerator mass spectrometry (AMS) (e.g., Ref. [12]) and inverse kinematics techniques [13]. These experiments were complemented by a number of theoretical studies based on empirical [14] and statistical model approaches [15]. These efforts have led to partially contradicting results, in particular with respect to the gamma counting and AMS measurements. To clarify the situation a number of experiments have been undertaken by the Notre Dame group to study the $^{40}\text{Ca}(\alpha, \gamma)^{44}\text{Ti}$ reaction using both methods. This first paper will present the results of a radiative capture measurement, which was performed with low-energy α beams from the RUBION Dynamitron accelerator at the Ruhr-Universität Bochum, Germany. A forthcoming second paper will focus on the results of an AMS study that was performed at the AMS facilities of the University of Notre Dame.

The following section will summarize previous experimental efforts and results. This will be followed by a description of the present experimental setup and the calibration measures taken for this experiment. The results will be discussed in the framework of a multiple resonance analysis. Finally the reaction rate will be derived from the experimental data and compared with previous experimental results and theoretical predictions.

II. PREVIOUS WORK

The $^{40}\text{Ca}(\alpha, \gamma)^{44}\text{Ti}$ reaction has been studied via different methods over the last 40 years. A previous series of prompt γ -ray studies measured a number of isolated narrow resonances

*drobert4@nd.edu

and identified many more [11,16–20] of interest. The main interest of most of these measurements, however, was focused on nuclear structure studies. It was the work of Cooperman, Shapiro, and Winkler [11] in 1977 that centered on the measurement of a reaction rate relevant for ^{40}Ca burning at stellar temperatures. In this work, calcium targets were evaporated *in situ* and prompt γ measurements were made of the 1083 keV decay line from the first excited state in ^{44}Ti as a result of α bombardment. The energy range of the experiment covered $E_\alpha = 2750\text{--}4000$ keV ($E_{\text{cm}} = 2500\text{--}3640$ keV) corresponding to $T = 1.2\text{--}2.1 \times 10^9$ K. In this range they identified and measured the resonance strengths of twelve isolated narrow resonances. The derived reaction rate was extended to a temperature of $T = 2.7 \times 10^9$ K by the inclusion of previously measured resonance strengths by Endt and Van der Leun [21]. Beyond these energies, Dixon, Storey, and Simpson [18] made further measurements at $E_\alpha = 3790\text{--}5950$ keV ($E_{\text{cm}} = 3450\text{--}5400$ keV), including the later identified strong triplet state at $E_x = 9215, 9227$, and 9239 keV ($E_{\text{cm}} \sim 4100$ keV) [19] (these studies are hereafter referred to as prompt gamma spectroscopy or PGS).

A more recent offline approach using AMS performed an integrated cross-section measurement over an extended energy range [12,22–24]. The experiment consisted of a helium gas cell under ^{40}Ca bombardment, with subsequent ^{44}Ti recoils implanted in a cooled copper catcher. The ^{44}Ti recoils were chemically separated from the copper and mixed with a titanium carrier material; the subsequent measurement of the ratio $^{44}\text{Ti}/^{\text{nat}}\text{Ti}$ via AMS provided an integrated resonance strength value. Two measurements were performed in this way: one over a small energy range centered on the strong triplet [24] and another over the range $E_{\text{cm}} = 2100\text{--}4200$ keV [12]. The smaller of the two energy ranges agrees well with the previous prompt γ -ray measurements. The larger however shows a significant increase in ^{44}Ti production. In developing a reaction rate for the AMS measurement, a scaled BRUSLIB (the Brussels Nuclear Library for Astrophysics Applications) [25] rate was modified to match the experimental averaged cross section of the full-range AMS measurement.

A later study by Vockenhuber *et al.* of the reaction over 100 isolated energy steps was performed using the DRAGON recoil mass separator [26,27]. The reaction was measured in inverse kinematics (in the following termed as IKS) using a ^{40}Ca beam incident on a windowless ^4He gas target [13]. The resultant recoils were separated by DRAGON and counted in a multinode ion chamber. Separate energy signals from the ion chamber were used for isobaric suppression; this was combined with γ -ray coincidence data from a BGO (bismuth germanate inorganic scintillator) array surrounding the ^4He gas cell. Two measurements were performed in this way: a preliminary activation over the strong triplet used to confirm the approach [28], then a wider range experiment covering $E_{\text{cm}} = 2110\text{--}4190$ keV (or $T = 1\text{--}2.8$ K), where 50 resonances were identified and resonance strengths measured. The reaction rate was determined from the deduced resonance strengths. A further six resonance contributions [29], at energies higher than those covered, were included in the final astrophysical reaction rate.

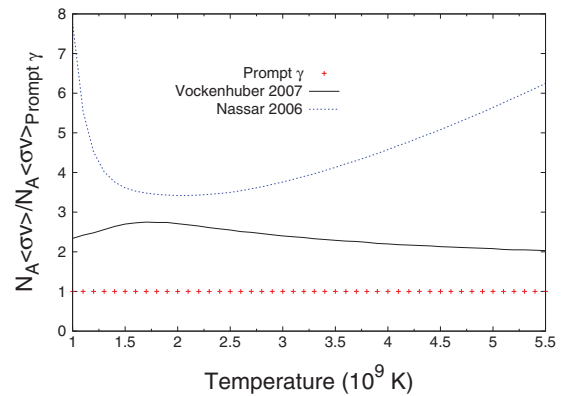


FIG. 1. (Color online) Reaction-rate predictions for $^{40}\text{Ca}(\alpha,\gamma)^{44}\text{Ti}$, based on AMS analysis (Nassar 2006) and IKS measurements (Vockenhuber 2007) in comparison the reaction-rate predictions based on the prompt gamma spectroscopy measurements outlined in the text.

Most recently a thick-target yield measurement was performed at the Lawrence Livermore National Laboratory (LLNL) Center for Accelerator Mass Spectrometry (CAMS) by Hoffman *et al.* [30]. An alpha beam incident on $^{\text{nat}}\text{CaO}$ was used for three thick-target yield measurements at $E_\alpha = 4.13, 4.54$, and 5.36 MeV. Prompt γ -ray data was collected for all three measurements, with a followup measurement of the $E_\alpha = 5.36$ MeV target via offline counting. A NON-SMOKER Hauser-Feshbach yield [31] was scaled down (by a factor of 1.71) to match the offline measurement, resulting in a “semiexperimental” astrophysical reaction rate.

The reaction rates predicted from the experimental results obtained by the different experiments show considerable discrepancies. Figure 1 shows the reaction rates normalized to the PGS rate based on all of the previously accumulated prompt gamma work discussed above. The PGS rate used in the figure is tabulated by Chen *et al.* [32]; a detailed analysis was also provided by Rauscher *et al.* 2000 [14]. In the astrophysically important region of a few 10^9 K, the reaction rate based the IKS studies is larger by a factor of 3 compared to the PGS rate, whereas the rate based on the AMS data shows a more significant enhancement by a factor of ~ 3.75 . These four approaches represent a significant cross section of measurements made, but not the study of this reaction in its entirety.

III. EXPERIMENTAL APPROACH

This work describes measurements performed at the RUBION Laboratory at the University of Bochum using a 12 inch \times 12 inch, single-crystal NaI(Tl) detector. The detector has a 35 mm diameter bore hole along its axis, resulting in a 98.9% coverage of 4π [33] for photons emitted from a target positioned at its center; see Fig. 2. The output of the six photomultiplier tubes (PMT) at the rear face of the detector were summed and fed into a single spectroscopy amplifier with a full scale energy range up to 14 MeV. The energy resolution at 10 MeV (near the maximum peak energy of interest for this work) was $\sim 2\%$.

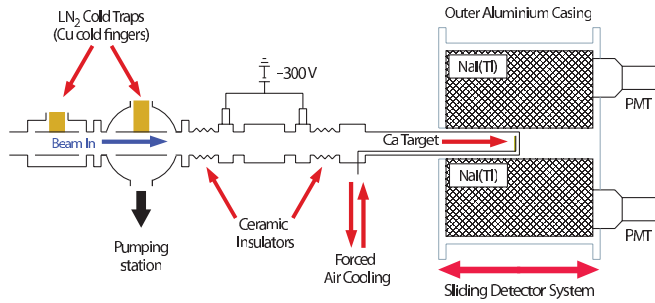


FIG. 2. (Color online) Detection layout for 12 inch \times 12 inch NaI(Tl) and associated beam line. The target is positioned to ensure full 4π coverage as shown in the configuration.

Two tantalum collimators (not shown in Fig. 2) located upstream of the target are used for beam tuning purposes and beam spot location; both are electrically isolated to optimize ion-beam focusing. The resultant beam spot diameter identified on the target is ~ 2 mm. A liquid-nitrogen-cooled copper tube of 400 mm length and 15 mm diameter separates the vacuum system of the target setup from the accelerator beam line. A second copper section also cooled to liquid-nitrogen temperatures ensures that no hydrocarbons from the pumping systems build up on the target during measurements. The end section of the beam line houses the target and holder; this section is electrically isolated to serve as a Faraday cup for a total integrated charge measurement. For the suppression of secondary electrons, a 300 V negative potential was applied at the front of this section (also electrically isolated from the remainder of the beam line). The target holder, which is constantly cooled through forced air cooling, is encapsulated in a stainless-steel vacuum pipe with a wall thickness of 0.5 mm, designed to minimize γ -ray absorption. The detector around the target is mounted to a carriage capable of sliding closer to or further from the beam line, providing variable γ -ray coverage.

The $^{40}\text{Ca}(\alpha, \gamma)^{44}\text{Ti}$ reaction has been studied with an incident $2 \mu\text{A}$ of $^4\text{He}^{2+}$ beam provided by the 4 MV Dynamitron tandem accelerator with the analyzing slits set to ± 2 mm. Targets were prepared by vacuum evaporation of metallic Ca, with a chemical purity of 99.5% and natural isotopic abundances, onto Cu backings. During the experiment targets of two different thicknesses were used, labeled “thick” and “thin” which correspond to target thicknesses or energy loss of a 4.5 MeV α beam [on a known $^{40}\text{Ca}(\alpha, \gamma)^{44}\text{Ti}$ resonance] of 52 ± 7 keV and 11.0 ± 1.5 keV respectively. The energy-loss values were obtained from the thick-target yield curve of the resonance. Due to the hydroscopic nature of calcium material, all targets were prepared fresh on-site with transportation and storage under argon atmosphere.

During target irradiation at the center of the NaI(Tl) detector, prompt γ rays from the interaction were measured with almost 4π coverage. The central positioning of the target and the use of a large volume detector allows for the use of the 4π γ -summing technique. The detection system in this configuration will generate a signal corresponding to the sum of all the γ decays of a cascade from a given entry state. Analysis of the resultant sum peak negates the

need for detailed γ -cascade information—something which may have handicapped the measurement of weak gamma branchings in previous PGS work—and moves the peak of interest (in energy) away from natural and beam induced background. With the detector’s 4π coverage there are no angular distribution corrections to be made, and the resulting reaction yield Y can be found from the measured sum-peak intensity I_Σ with the following relation:

$$Y = \frac{I_\Sigma}{N_b \varepsilon_\Sigma}. \quad (1)$$

Here N_b is the number of incident particles and ε_Σ is the sum-peak efficiency as determined via the process outlined in Sec. III A.

Due to the relatively large detector efficiency, it is possible to measure the reaction of interest with low incident beam currents, increasing the longevity of the fragile calcium targets. However, prolonged helium bombardment during a thick-target yield measurement makes possible target degradation a major concern. Monitoring target stability in this work consisted of multiple target scans over the strong resonance triplet at $E_x \sim 9.2$ MeV.

A. Efficiency measurements

In principle the summing method is straightforward. It has a high detection efficiency, is independent of the angular distribution, and does not depend in first order on the exact γ -decay branchings of the reactions. However, the absolute summing efficiency does depend on the multiplicity M of the decay. A higher multiplicity will result in a lower sum-peak efficiency as the probability of a photon escaping the detector is increased, precluding that event from being included in the resultant sum peak.

The lack or difficulty of extracting γ -branching information requires an alternative method for determining the average multiplicity $\langle M \rangle$. Spyrou *et al.* [34] developed the “in/out” ratio method, which considers two target positioning extremes relative to the NaI detector. With a target positioned at the center of the detector it can be assumed ideally that all γ emissions are collected and contribute to the sum-peak intensity I_{in} . A similar measurement performed with the target at the entrance of the detector results in a sum-peak intensity I_{out} (a comparison of which can be seen in Fig. 3) which can be described for an ideal case by $I_{\text{out}} = I_{\text{in}}/2$. The ratio between the two,

$$R = \frac{I_{\text{in}}}{I_{\text{out}}}, \quad (2)$$

for a single emitted photon in a decay would therefore be $R = 2$. Conversely, for reactions of multiplicity $M = 2, 3$, and 4 one would have corresponding values of $R = 4, 8$, and 16 respectively, reducing simply to the relation $R = a^M$, where $a = 2$ is for an ideal case. Hence, the ratio method can be used to determine the average multiplicity $\langle M \rangle$ of the reaction of interest. Considerable work by Spyrou *et al.* [34] has gone

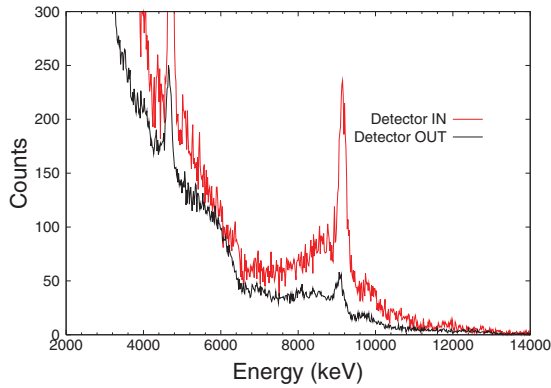


FIG. 3. (Color online) γ spectra shown for the $^{40}\text{Ca}(\alpha,\gamma)^{44}\text{Ti}$ reaction with $E_\alpha = 4450$ keV. The upper spectra labeled “IN” was measured with the target at the center of the detector and the lower spectra labeled “OUT” with the target at the entrance; see Fig. 2.

into quantifying this relation for the experimental setup used in this work as $R = 2.48(3)^{\langle M \rangle}$.

Average multiplicities found from extensive characterization of the detector using known sources, measured reactions, and detailed γ -branching information have previously been used in sum-peak efficiency determination. Here the sum-peak efficiency values $\varepsilon_{M=x}$ and $\varepsilon_{M=x+1}$ are calculated by a Monte Carlo simulation using the code GEANT4 [35]. Simulations for integer values of M can be found in Fig. 10 of Ref. [34], where shaded regions represent the uncertainties obtained via arbitrarily varying the individual γ energies composing the sum-peak energy; this results in no available uncertainty contribution from $M = 1$. These values can then be related to the sum-peak efficiency for an average multiplicity $\langle M \rangle$ of the form $\langle M \rangle = x.yz$,

$$\varepsilon_{\langle M \rangle} = (1 - 0.yz) \times \varepsilon_{M=x} + 0.yz \times \varepsilon_{M=x+1}. \quad (3)$$

It must be noted that this combination of efficiencies is merely a convention that has been adopted from Ref. [34] for

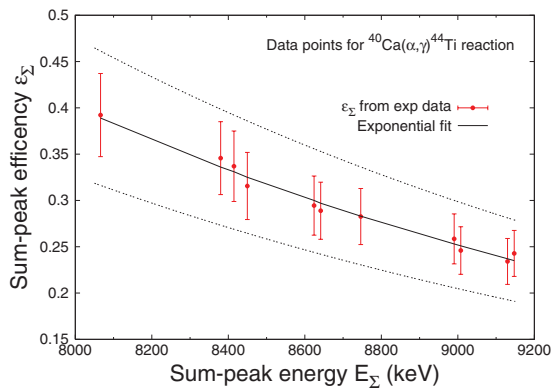


FIG. 4. (Color online) Sum-peak efficiencies obtained from experimental ratio measurements taken for the $^{40}\text{Ca}(\alpha,\gamma)^{44}\text{Ti}$ capture reaction. The solid line represents the fit of a single exponential function, with the upper and lower dotted lines representing a $\pm 1\sigma$ band.

transparency reasons, and that multiple other combinations of both efficiencies and multiplicities are possible for an ultimate efficiency determination for $\langle M \rangle$.

The energy dependence between the calculated ε_Σ from Eq. (3) and the sum-peak energy E_Σ can be described by a function of the form

$$\varepsilon_\Sigma = \varepsilon_0 + a \exp(-E_\Sigma/b). \quad (4)$$

This relation is shown in Fig. 4 for values of the sum-peak efficiency calculated from 11 measurements of $\langle M \rangle$ for the specific case of the $^{40}\text{Ca}(\alpha,\gamma)^{44}\text{Ti}$ reaction performed as a part of this work. Both the “IN” and “OUT” configurations have been utilized along with Eq. (2); this relation has been used with the parameters $a = 16.6 \pm 3.1$ and $b = (4.65 \pm 0.21) \times 10^{-4}$ (from Fig. 4) where $\langle M \rangle$ is unknown.

IV. RESULTS AND DISCUSSION

Assuming that the target thickness is large compared to the total width of a resonance, the resonance strength ($\omega\gamma$) can be determined from the reaction yield Y using the familiar thick-target relation

$$\omega\gamma = Y \frac{2\varepsilon}{\lambda^2} \left(\frac{m_t}{m_t + m_p} \right), \quad (5)$$

where the stopping power (ε) in the laboratory system, target and projectile masses (m_t and m_p), and the de Broglie wavelength (λ) in the center-of-mass system are also required.

A. Excitation function

An excitation function has been measured between $E_\alpha = 3.0$ and 4.6 MeV ($E_{\text{cm}} = 2.72$ and 4.18 MeV) in 10 keV steps using the thick target, and is shown in Fig. 5. In addition some measurements were taken with the thin target to resolve doublets; see the inset of Fig. 5. Where resonances could not be resolved the yield represents the sum of the individual contributions. The solid line is a MINUIT fit to the data based on

$$Y(E_\alpha) = \frac{\lambda_r^2 \omega\gamma}{2\pi \varepsilon} \left[\arctan \left(\frac{E_\alpha - E_r}{\Gamma/2} \right) - \arctan \left(\frac{E_\alpha - E_r - \Delta E}{\Gamma/2} \right) \right], \quad (6)$$

where ε is the stopping power, E_α is the beam energy, Δ is the energy loss in the target, λ_r is the de Broglie wavelength at a given resonance energy, and Γ is the resonance width. Resonance parameters $\omega\gamma$ and E_r for identified regions of interest were allowed to vary within $\pm 10\%$ of measured values for a best fit to all data points; resulting values are listed in Table I. The uncertainties from the MINUIT fit for the resonance parameters have been adjusted to include the 5% uncertainty in the stopping power and then added in quadrature with uncertainties generated for the detector efficiency.

To ensure the excitation function is independent of target properties, the absolute resonance strengths of the reactions

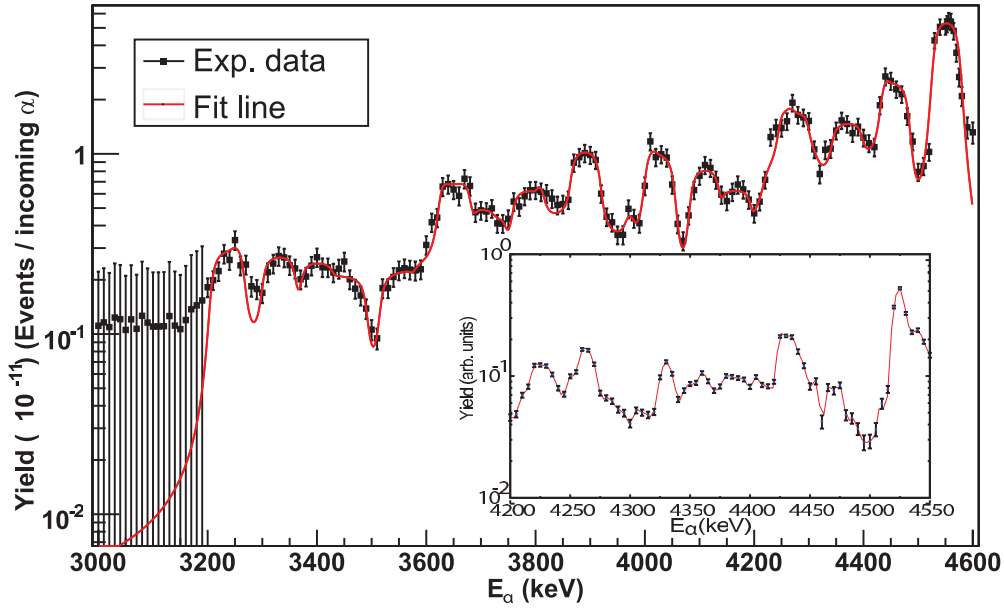


FIG. 5. (Color online) Yield curve measured over the energy range $E_\alpha = 3000\text{--}4600$ keV. Both experimental data points and the MINUIT fit line are shown. Data points in the energy region below 3200 keV are displayed as upper limits only. The inset shows the yield curve of the thin target over the energy range $E_\alpha = 4200\text{--}4550$ keV.

were determined relative to the well known strength of the 1.84 MeV resonance in the reaction $^{40}\text{Ca}(p,\gamma)^{41}\text{Sc}$, which was measured in identical conditions to the strong triplet in the

TABLE I. Resonance parameters as extracted by the MINUIT fitting routine based on Eq. (6).

E_{res} (keV)	E_x (keV)	$\omega\gamma$ (eV)
4116 ± 1.4	9243 ± 1.4	8.994 ± 1.170
4028 ± 1.7	9155 ± 1.7	3.709 ± 0.684
3991 ± 5.1	9118 ± 5.1	0.810 ± 0.128
3948 ± 2.5	9076 ± 2.5	2.100 ± 0.328
3920 ± 5.6	9046 ± 5.6	0.798 ± 0.123
3871 ± 1.4	8999 ± 1.4	1.571 ± 0.247
3836 ± 2.1	8964 ± 2.1	2.128 ± 0.340
3768 ± 2.6	8895 ± 2.6	1.349 ± 0.213
3711 ± 1.9	8838 ± 1.9	0.685 ± 0.105
3636 ± 1.3	8763 ± 1.3	1.221 ± 0.195
3601 ± 3.7	8728 ± 3.7	0.297 ± 0.047
3568 ± 3.4	8695 ± 3.4	0.185 ± 0.028
3512 ± 1.7	8639 ± 1.7	1.773 ± 0.235
3442 ± 2.9	8569 ± 2.9	0.794 ± 0.119
3396 ± 3.4	8524 ± 3.4	0.639 ± 0.102
3338 ± 2.3	8465 ± 2.3	0.496 ± 0.078
3293 ± 2.5	8419 ± 2.5	0.667 ± 0.103
3255 ± 3.0	8382 ± 3.0	0.471 ± 0.076
3193 ± 2.0	8320 ± 2.0	0.190 ± 0.030
3127 ± 1.8	8254 ± 1.8	0.119 ± 0.018
3110 ± 3.6	8237 ± 3.6	0.050 ± 0.008
3068 ± 3.0	8195 ± 3.0	0.395 ± 0.063
3007 ± 2.3	8134 ± 2.3	0.157 ± 0.025
2995 ± 6.9	8123 ± 6.9	0.109 ± 0.018
2945 ± 2.3	8072 ± 2.3	0.090 ± 0.014
2910 ± 2.7	8036 ± 2.7	0.467 ± 0.074

$^{40}\text{Ca}(\alpha,\gamma)^{44}\text{Ti}$ reaction with evaporated calcium on tantalum backings. The measured strength for the 1.84 MeV resonance in this work (0.28 ± 0.04) eV agrees well with the documented (0.28 ± 0.03) eV value [36]. Review of the strong resonance triplet gives a fit value of integrated resonance $\omega\gamma_{\text{int}} = 9.0 \pm 1.2$ eV, showing good agreement to the literature value of 8.5 ± 1.1 eV [32] and previous measurements of 7.6 ± 1.0 eV [13] and 8.8 ± 3.0 eV [12]. The $\omega\gamma$ value for this triplet is reliably consistent for all scans made during target degradation monitoring, giving increased confidence in the procedure.

Measurements below $E_\alpha = 3.2$ MeV can only be considered as upper limits due to a lack of discernible sum-peak information during spectral analysis. This information has not been included in reaction-rate calculations outlined later.

B. Reaction-rate calculation

The astrophysical reaction rate of $^{40}\text{Ca}(\alpha,\gamma)^{44}\text{Ti}$ given in Table II is calculated from the relation

$$N_A \langle \sigma v \rangle = \frac{1.54 \times 10^{11}}{(\mu T)^{3/2}} \sum_{i=1}^N (\omega\gamma)_i \exp\left(-\frac{11.605 E_i}{T}\right), \quad (7)$$

with the reduced mass μ in amu and T is the temperature in GK. The values of the resonance strengths $\omega\gamma$ and resonance energies E_r taken from Table I are in units of MeV. This rate is graphically represented in Fig. 6 compared to previous experimental work (outlined in Sec. II) and a selection of statistical models in Fig. 7. Insets in both figures show comparisons of the previously derived reaction rates normalized to the rate presented in this work. The shape of the present reaction rate most visibly alters when contrasted against literature values below a temperature of 1.5×10^9 K.

TABLE II. $^{40}\text{Ca}(\alpha,\gamma)^{44}\text{Ti}$ reaction rate, including rate and limits established from excitation function fit and reaction rate including extra resonance values.

T (GK)	Reaction rate $N_A\langle\sigma v\rangle$ ($\text{cm}^3\text{s}^{-1}\text{mol}^{-1}$)			
	NON-SMOKER	Lower limit	Complete rate	Upper limit
0.1	2.27×10^{-47}			
0.15	2.07×10^{-38}			
0.2	9.10×10^{-33}			
0.3	1.03×10^{-25}			
0.4	2.72×10^{-21}			
0.5	3.59×10^{-18}			
0.6	8.20×10^{-16}			
0.7	6.03×10^{-14}			
0.8	2.01×10^{-12}			
0.9	3.78×10^{-11}			
1.0	4.60×10^{-10}	8.06×10^{-11}	1.03×10^{-10}	1.26×10^{-10}
1.5	2.31×10^{-6}	2.13×10^{-6}	2.63×10^{-6}	3.16×10^{-6}
2.0	3.49×10^{-4}	4.50×10^{-4}	5.48×10^{-4}	6.50×10^{-4}
2.5	9.53×10^{-3}	1.21×10^{-2}	1.46×10^{-2}	1.72×10^{-2}
3.0	9.81×10^{-2}	1.12×10^{-1}	1.35×10^{-1}	1.59×10^{-1}
3.5	5.45×10^{-1}	5.61×10^{-1}	6.76×10^{-1}	7.93×10^{-1}
4.0	2.00	1.89	2.27	2.66
4.5	5.50	4.85	5.82	6.82
5.0	1.23×10^1	1.03×10^1	1.23×10^1	1.44×10^1
5.5	2.35×10^1	1.89×10^1	2.27×10^1	2.66×10^1

When compared to previous rates, the steeper drop-off at low energy is possibly due to a lack of information on resonances in this region, as depicted by the upper-limit values in Fig. 5. Due to the lack of measurements outside the $E_\alpha = 3.0\text{--}4.6$ MeV range of this work, some previously measured resonance information (only one resonance at lower energy and six at higher energies are available) has been included in the reaction-rate calculations [36]. Table II lists the calculated reaction rate, including upper and lower limits. Limits were obtained by taking the maximal and minimal values of the calculated resonance parameters entered into Eq. (7). Also shown in Table II is a NON-SMOKER calculation (described later and shown in Fig. 7) for the reaction rate that extends to lower temperatures than this work. This rate was chosen for a description of the rate below 1×10^9 K due to the good agreement with this work in the $1\text{--}5.5 \times 10^9$ K range.

As with more recent measurements, this work gives a rate larger than that of the original PGS data, where a reaction rate has been calculated using resonances identified in the previously discussed studies of Refs. [11,16–20]. This difference is due in part to the significant increase in identified resonance structure, previously also noted in Ref. [13]. In the temperature range $>1.5 \times 10^9$ K there is good agreement (within quoted limits) between this work and the IKS work [13], which is smaller by a factor of 1.33. Conversely the AMS [12] rate is greater by an average factor of 1.44 with an increasingly larger deviation visible above $T = 3.5 \times 10^9$ K. The PGS work is smaller by an average factor of 3.3. The reaction-rate work by Hoffman *et al.* [30] is slightly different due to the use of a normalized theoretical cross section for their

reaction-rate calculations. From this they stress an assigned factor-of-2 uncertainty in their rate (not shown on figure comparisons), bringing it possibly much closer to the measured rate in this work.

Beyond previous experimental approaches, there are many statistical model calculations available for the the $^{40}\text{Ca}(\alpha,\gamma)^{44}\text{Ti}$ reaction based on the Hauser-Feshbach approach [15], which gives reliable predictions if the level density in the compound nucleus is high enough, which is usually the case for nuclei heavier than around mass 40 and close to the valley of stability. In Fig. 7 a comparison has been made to results from the statistical model code NON-SMOKER as outlined in the Reaclib database [37] (and listed in Table II), and BRUSLIB data based on the TALYS approach [38–41]. Included also in the comparison is the empirical approach by Rauscher *et al.* [14]. The best reproduction of the rate from this work is by NON-SMOKER, with some slight differences in shape below 1.5×10^9 K. Similar behavior is demonstrated by the BRUSLIB rate, with a region of closer similarity than the NON-SMOKER rate at a temperature of 2×10^9 K, but with much greater deviation in the range below 1.5×10^9 K and above 3×10^9 K. The Rauscher empirical rate shows the most similarity to this work but underpredicts by a factor of ~ 2.4 . The underprediction by this last rate can be understood when considering that it was formed in comparison to experimental values current at the time. The differing behavior of the empirical and purely statistical calculations stems from the treatment of the isospin selection rule for $E1$ transitions ($\Delta T = 0, 1$), which strongly suppresses (α,γ) capture reactions on self-conjugate ($N = Z$, $T = 0$) nuclei. The inclusion of more isospin data resulted in lower predicted

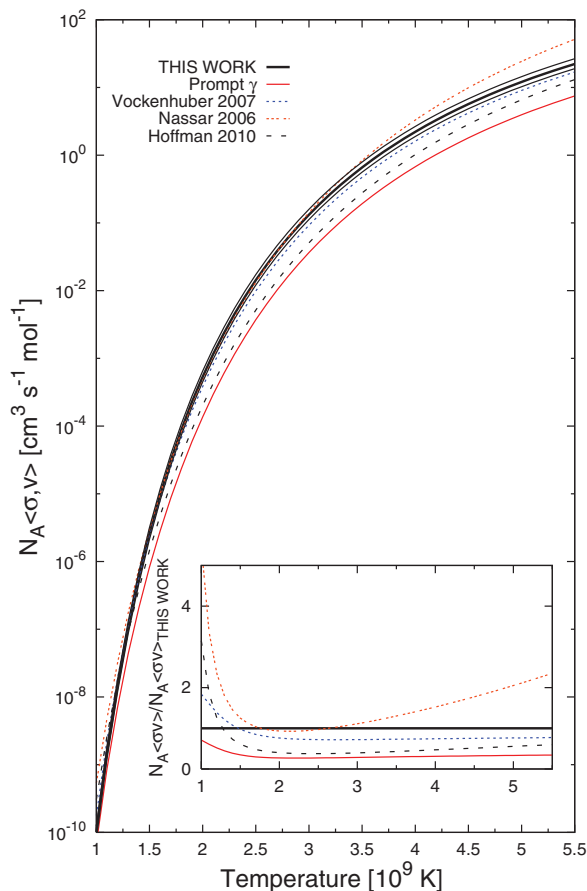


FIG. 6. (Color online) Stellar reaction rate as a function of temperature. Rates from experimental approaches outlined in Sec. II are shown in comparison with this work. This work is displayed with solid bounding lines for upper and lower limits. The inset shows rates normalized to this work; all references for these rates are given in the text.

reaction rates for all but one of the reactions studied in Ref. [14].

V. CONCLUSIONS

In this work resonance energies and resonance strengths for the $^{40}\text{Ca}(\alpha, \gamma)^{44}\text{Ti}$ reaction have been extracted from an excitation function measured over the energy range $E_\alpha = 3.0\text{--}4.6$ MeV. These parameters have then been used to determine the reaction rate. The use of a well characterized 4π NaI detector has made measurements independent of angular corrections. Absolute resonance strengths have been determined relative to the well known 1.84 MeV resonance in the $^{40}\text{Ca}(p, \gamma)^{41}\text{Sc}$ reaction. Comparison with the well established ~ 9.2 MeV resonance triplet has shown good agreement with previous work [13].

We find that previous PGS measurements [11,16–20] are approximately a factor of 3.3 smaller than our reaction rate over the astrophysically relevant temperature range of $T = 1\text{--}5.5 \times 10^9$ K. However our rate lies between the more recently published results of AMS and offline counting

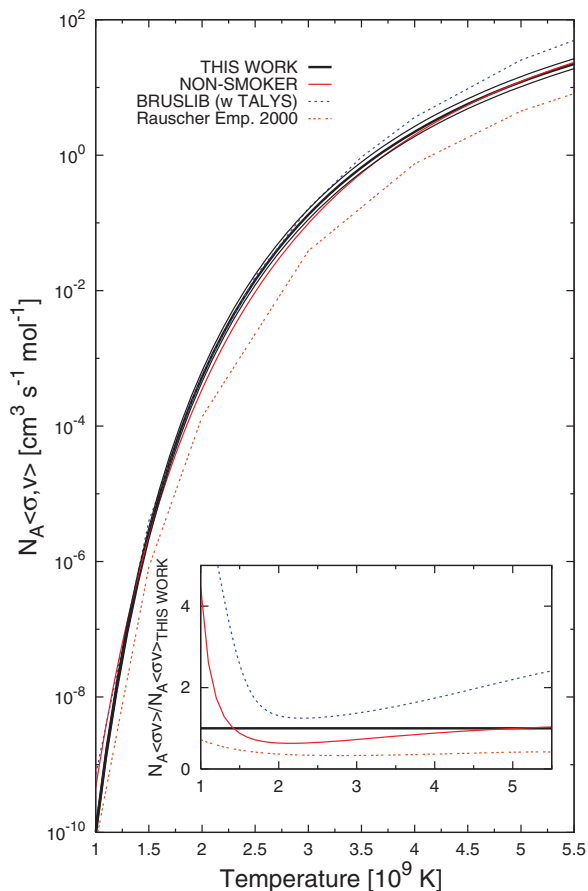


FIG. 7. (Color online) Stellar reaction rate as a function of temperature. This work is compared against some current statistical model calculations of interest. This work is displayed with solid bounding lines for upper and lower limits. The inset shows rates normalized to this work; all references for these rates are given in the text.

measurements outlined in Ref. [12,30]. Our rate also shows close agreement with the IKS studies outlined in Ref. [13] which is smaller on average by a factor of 1.33, and, similar to this work, indicates an increase in identified resonance structure. Even though our new rate represents an approximate factor-of-3 increase over the prompt- γ measurements, it is unlikely to account for observed discrepancies between simulated and observational ^{44}Ti production in supernova remnants.

ACKNOWLEDGMENTS

The authors would like to thank the RUBION operator team for their outstanding technical support throughout the experiment. A special thanks also to R. D. Hoffman for many enlightening and constructive discussions during this work. Acknowledgment and thanks must also be given to the support of the National Science Foundation (Grant No. PHYS-58100) and the Joint Institute for Nuclear Astrophysics (Grant No. PHY08-22648).

- [1] R. Diehl, H. Halloin, K. Kretschmer, G. G. Lichti, A. W. S. V. Schönfelder, A. von Kienlin, W. Wang, P. Jean, J. Knödseder, J.-P. Roques *et al.*, *Nature (London)* **439**, 45 (2006).
- [2] A. F. Iyudin, R. Diehl, H. Bloemen, W. Hermsen, G. G. Lichti, D. Morris, J. Ryan, V. Schönfelder, H. Steinle, M. Warendorf *et al.*, *Astron. Astrophys.* **284**, L1 (1994).
- [3] A. F. Iyudin, Schönfelder, K. Bennett, H. Bloemen, R. Diehl, W. Hermsen, G. G. Lichti, R. D. van der Meulen, J. Ryan, and C. Winkler, *Nature (London)* **396**, 142 (1998).
- [4] F. X. Timmes, S. E. Woosley, D. H. Hartmann, and R. D. Hoffman, *Astrophys. J.* **464**, 332 (1996).
- [5] P. A. Young, C. L. Fryer, A. Hungerford, D. Arnett, G. Rockefeller, F. X. Timmes, B. Voit, C. Meakin, and K. A. Eriksen, *Astrophys. J.* **640**, 891 (2006).
- [6] P. A. Young and C. L. Fryer, *Astrophys. J.* **664**, 1033 (2007).
- [7] S. E. Woosley and R. D. Hoffmann, *Astrophys. J.* **395**, 202 (1992).
- [8] L.-S. The, D. D. Clayton, L. Jin, and B. S. Meyer, *Astrophys. J.* **504**, 500 (1998).
- [9] R. D. Hoffman, S. A. Sheets, J. T. Burke, N. D. Scielzo, T. Rauscher, E. B. Norman, S. Tumey, T. A. Brown, P. G. Grant, A. M. Hurst *et al.*, *Astrophys. J.* **715**, 1383 (2010).
- [10] G. Magkotsios, F. X. Timmes, A. L. Hungerford, C. L. Fryer, P. A. Young, and M. Wiescher, *Astrophys. J. Suppl.* **191**, 66 (2010).
- [11] E. L. Cooperman, M. H. Shapiro, and H. Winkler, *Nucl. Phys. A* **284**, 163 (1977).
- [12] H. Nassar, M. Paul, I. Ahmad, Y. Ben-Dov, J. Caggiano, S. Ghelberg, S. Goriely, J. P. Greene, M. Hass, A. Heger *et al.*, *Phys. Rev. Lett.* **96**, 041102 (2006).
- [13] C. Vockenhuber, C. O. Ouellet, L.-S. The, L. Buchmann, J. Caggiano, A. A. Chen, H. Crawford, J. M. D'Auria, B. Davids, L. Fogarty *et al.*, *Phys. Rev. C* **76**, 035801 (2007).
- [14] T. Rauscher, F. K. Thielemann, J. Görres, and M. Wiescher, *Nucl. Phys. A* **675**, 695 (2000).
- [15] W. Hauser and H. Feshbach, *Phys. Rev.* **87**, 366 (1952).
- [16] J. J. Simpson, W. R. Dixon, and R. S. Storey, *Phys. Rev. C* **4**, 443 (1971).
- [17] R. E. Peschel, J. M. Long, H. D. Shay, and D. A. Bromley, *Nucl. Phys. A* **232**, 269 (1974).
- [18] W. R. Dixon, R. S. Storey, and J. J. Simpson, *Phys. Rev. C* **15**, 1896 (1977).
- [19] W. R. Dixon, R. S. Storey, and J. J. Simpson, *Can. J. Phys.* **58**, 1360 (1980).
- [20] W. R. Dixon, R. S. Storey, and A. F. Bielajew, *Nucl. Phys. A* **378**, 273 (1982).
- [21] P. M. Endt and C. van der Leun, *Nucl. Phys. A* **214**, 1 (1973).
- [22] S. K. Hui, M. Paul, D. Berkovits, E. Boaretto, S. Ghelberg, M. Hass, A. Hershkowitz, and E. Navon, *Nucl. Instrum. Methods B* **172**, 642 (2000).
- [23] H. Nassar, M. Paul, S. Ghelberg, A. Ofan, N. Trubnikov, Y. Ben-Dov, M. Hass, and B. N. Singh, *Nucl. Phys. A* **758**, 411 (2005).
- [24] M. Paul, C. Feldstein, I. Ahmad, D. Berkovits, C. Bordeanu, J. Caggiano, S. Ghelberg, J. Goerres, J. Greene, M. Hass *et al.*, *Nucl. Phys. A* **718**, 239 (2003).
- [25] M. Arnould and S. Goriely, *Nucl. Phys. A* **777**, 157 (2006).
- [26] S. Engel, D. Hutcheon, S. Bishop, L. Buchmann, J. Caggiano, M. Chatterjee, A. Chen, J. D'Auria, D. Gigliotti, U. Greife *et al.*, *Nucl. Instrum. Methods Phys. Res., Sect. A* **553**, 491 (2005).
- [27] D. A. Hutcheon, S. Bishop, L. Buchmann, M. L. Chatterjee, A. A. Chen, J. M. D'Auria, S. Engel, D. Gigliotti, U. Greife, D. Hunter *et al.*, *Nucl. Instrum. Methods Phys. Res., Sect. A* **498**, 190 (2003).
- [28] C. Vockenhuber, C. Ouellet, L. Buchmann, J. Caggiano, A. Chen, J. D'Auria, D. Frekers, A. Hussein, D. Hutcheon, W. Kutschera *et al.*, *Nucl. Instrum. Methods Phys. Res., Sect. B* **259**, 688 (2007).
- [29] J. A. Cameron and B. Singh, *Nucl. Data Sheets* **88**, 299 (1999).
- [30] R. D. Hoffman, S. A. Sheets, J. T. Burke, N. D. Scielzo, T. Rauscher, E. B. Norman, S. Tumey, T. A. Brown, P. G. Grant, A. M. Hurst *et al.*, *Astrophys. J.* **715**, 1383 (2010).
- [31] T. Rauscher and F.-K. Thielemann, *At. Data Nucl. Data Tables* **79**, 47 (2001).
- [32] J. Chen, B. Singh, and J. A. Cameron, *Nucl. Data Sheets* **112**, 2357 (2011).
- [33] A. Best, Diploma Thesis, Ruhr-Universität Bochum, Germany (unpublished).
- [34] A. Spyrou, H.-W. Becker, A. Lagoyannis, S. Harissopoulos, and C. Rolfs, *Phys. Rev. C* **76**, 015802 (2007).
- [35] S. Agostinelli *et al.*, *Nucl. Instrum. Methods Phys. Res., Sect. A* **506**, 250 (2003).
- [36] P. M. Endt, *Nucl. Phys. A* **521**, 1 (1990).
- [37] R. H. Cyburt, A. M. Amthor, R. Ferguson, Z. Meisel, K. Smith, S. Warren, A. Heger, R. D. Hoffman, T. Rauscher, A. Sakharuk *et al.*, *Astrophys. J. Suppl. Ser.* **189**, 240 (2010).
- [38] A. J. Koning, S. Hilaire, and M. Duijvestijn, NRG Report No. 21297/04.62741/P, 2004.
- [39] A. J. Koning, S. Hilaire, and M. Duijvestijn, in *Proceedings of the International Conference on Nuclear Data for Science and Technology, Nice, 2007*, edited by O. Bersillon *et al.* (EDP Sciences, Les Ulis, France, 2008).
- [40] S. Goriely, S. Hilaire, and A. J. Koning, *Astron. Astrophys.* **487**, 767 (2008).
- [41] S. Goriely, S. Hilaire, A. J. Koning, M. Sin, and R. Capote, *Phys. Rev. C* **79**, 024612 (2009).